Assiut University Journal of Multidisciplinary Scientific Research (AUNJMSR)
Faculty of Science, Assiut University, Assiut, Egypt.
Printed ISSN 2812-5029
Online ISSN 2812-5037
Vol. 52(1): 67- 97 (2023)
https://aunj.journals.ekb.eg/

Environmental assessment of heavy metals contamination in Sharm El Madfa and Abu Ramad coastal sediments, Red Sea, Egypt

Mamdouh Soliman[1*], Nageh Obaidalla1, Islam El-Sheikh[2], Fatma Elzahra Bakheet[1], Mohamed Abdel-Wahab[3]

1Geology Department, Faculty of Science, Assiut University, Egypt

2Geology Department, Faculty of Science, Al Azhar University, Assiut Branch, Egypt

3Late Professor, National Institute of Oceanography and Fisheries, Red Sea Branch, Hurghada, Egypt

*Corresponding author: e-mail: solimann@aun.edu.eg; msoliman20032003@yahoo.com

ARTICLE INFO

Article History:
Article History:
Received: 2022-11-23
Accepted: 2022-12-13
Online: 2022-12-29

Keywords: Pollution indicators, Contamination degree , Mangrove swamp, Anthropogenic sources, Heavy metals.

.

ABSTRACT

To assess the contamination levels of selected heavy metals of the Sharm El Madfa and Abu Ramad coastal sediments, Red Sea, Egypt, 22 bottom sediment samples were collected from the two sites. The concentrations of the heavy metals were recorded using inductively coupled plasma emission spectrometer (ICP-ES) technique. The level of pollution was evaluated using both single and integrated pollution indices. Moreover, statistical (correlation) analyses were performed. The geo-accumulation index, contamination factor, contamination degree, and pollution load index showed that the sediments at both sites were unpolluted. However, the enrichment factor shows higher values for all metals (EF > 1.5). These values of EF indicate that these metals are slightly to moderately severe enriched relative to the background and suggest that some fractions of the sources of these metals are more likely to be anthropogenic. The improved Nemerow index values indicate that the overall level of heavy metal contamination in the studied sediments of the two sites is between heavily and extremely contaminated. The calculated anthropogenic fraction percentages for Fe, Mn, Cu, Zn, Ni, As, V and Cr show various proportions among all metals of the sediments. The correlation between the heavy metals with both of Al, Si and Ti indicates that these metals are associated with the detrital charier phases and/or absorbed by iron and Mn-oxides and or hydroxides. The possible anthropogenic sources of these metals are shipment operations and anticorrosive and antifouling paints, dredging and land filling, municipal wastewater from tourist centers and fishermen cargo boats.

INTRODUCTION

The Red Sea is a semi-closed sea, which separates the African and Arabian plates. It communicates with the Indian Ocean by the Gulf of Aden at its southern end. The Red Sea is characterized by warm temperatures and more saline water. The Egyptian shoreline is characterized by the occurrences of different morphological features such as bays (sharms), lagoons and swamps. It also contains manufactured buildings such as fisher centers, petroleum harbors and tourist centers. Generally, the different environments in the shoreline of the seas subject to different sources of heavy metals pollution of anthropogenic activities. Heavy metal pollutants find their way into coastal marine environments through a variety of sources, including industrial and mining and urban activities, agricultural, wastewater and domestic effluents generated by coastal cities and resorts [1-3].

The shoreline environments of the seas are the nearest areas, which receive the different types of the contaminants. These contaminants precipitate along with the surface sediments. There are different types of biota living within the sediments such as algae, foraminifera, mollusca, coral and echinodermata. The heavy metals are the most widespread and hazardous environmental pollutants that have to contaminate the fresh, brackish and marine water environments [4]. The contamination related with metals is a serious problem due to their toxicity and their tendency to accumulate in biota. They cause negative effects on the different biota in the environments [5,6], and concurrently, the heavy metals affect human health [7]. The most critical properties of metals are that they are not biodegradable in the environment and undergo a global ecological cycle [8-12].

The contamination of coastal sediments with heavy metals has become a severe problem, especially in regions of population increase and urban expansion. Several investigations on heavy metal pollutants have been reported on coastal sediments and marine skeletons of the Red Sea (e.g. [2, 13-22]). Sediments serve as a reservoir of metals that could be liberated to the overlying water from natural and anthropogenic processes

such as bioturbation and dredging, resulting in potential adverse unfavorable health effects [23, 24].

The current study therefore, aimed to: (1) determine the distribution and concentration of trace metals in bottom sediments from 22 stations in the recent sediments at two shoreline environments in the southern part of the Egyptian Red Sea (Sharm El-Madfa and Abu Ramad, Fig. 1); and (2) to assess the extent and degree of metals, and the origin of these metals, using both single and integrated pollution indices of the metals. Sharm El-Madfa represents a swamp environment, however, Abu Ramad represents a fishing center for its dwelling peoples (Fig. 2).

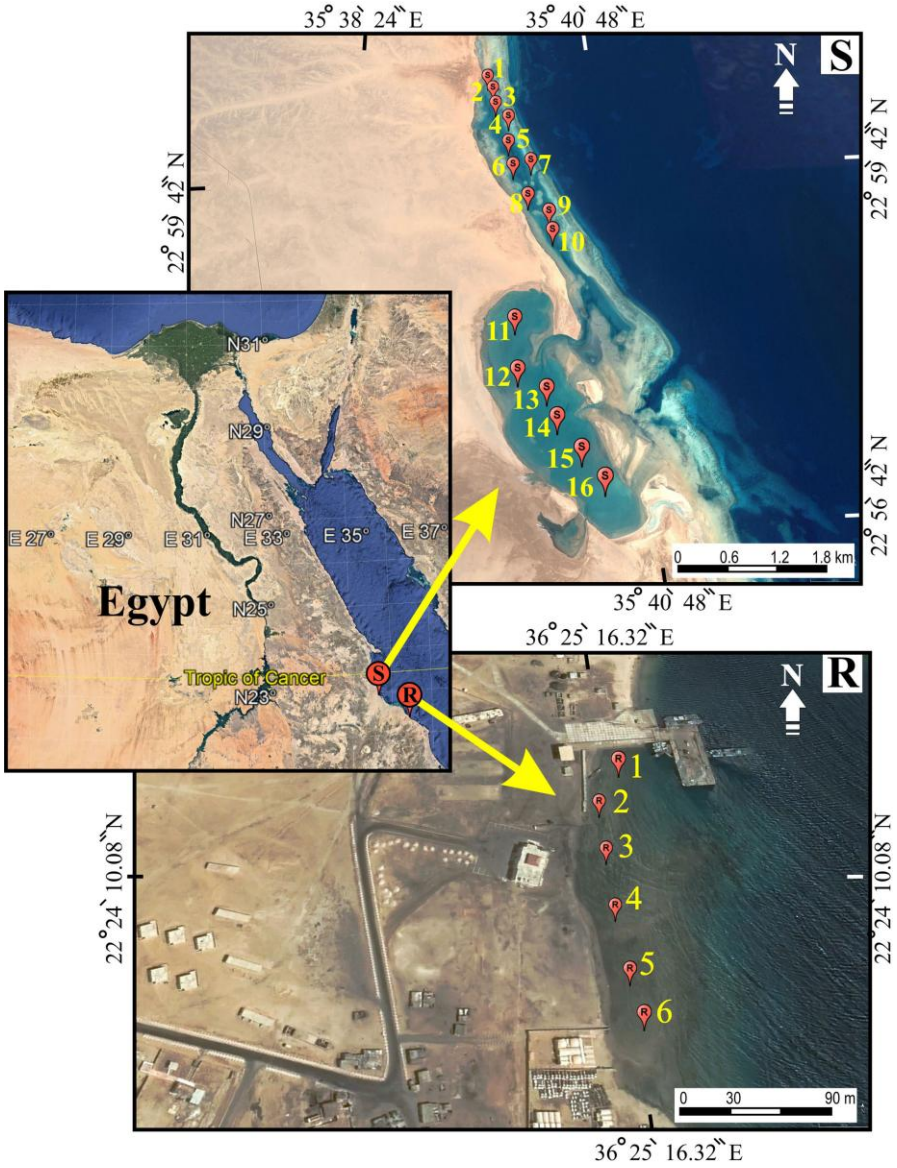

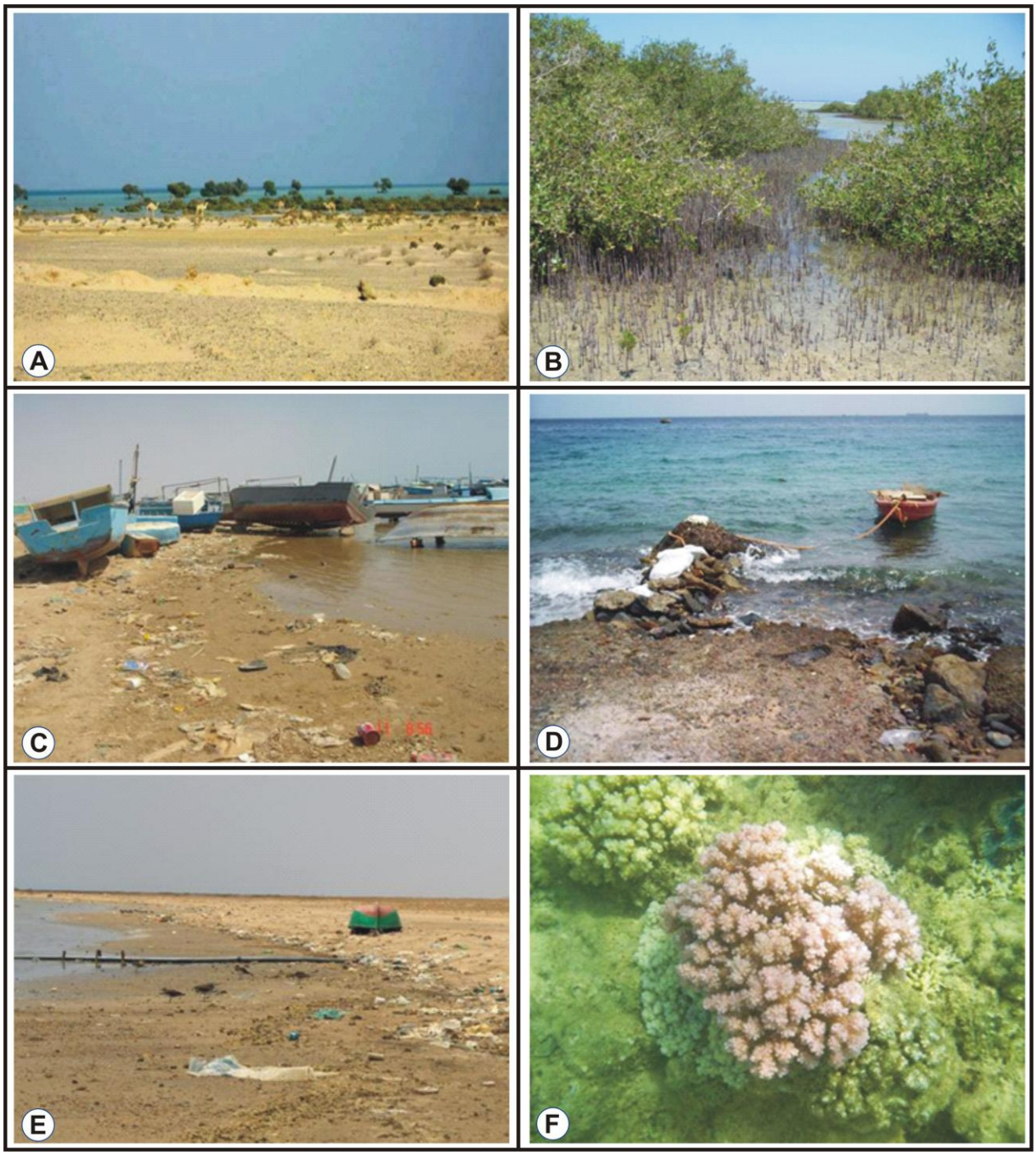

Figure 1. Location map of the Sharm El Madfa (S) and Abu Ramad (R) coastlines and the locations of sediment samples along the coast.

Figure 2. Field photographs showing some sources of pollutants in the study sites, (A & B) The mangrove swamp and animal waste along the coast of Sharm El Madfa site, (C &

D) Solid wastes of a fishing boats along the Abu Ramad coast, (E) Solid wastes and pouring of wastewater directly on the beach, (F) Coral reefs with some sea grass (Abu Ramad coast).

Materials and methods

Sites Description

1. Sharm El Madfa site

Sharm El Madfa site is considered a big mangrove swamp mainly composed of *Avicennia marina* and *Rhizophoramucronata*. It represents a semi-closed area with a small inlet. It is located 37 km south of Shalatein city between latitude 22°02′22.0″-22°56′58″N and longitude 35°39′30.0″-35°41′70.0″E (Fig. 1). This swamp is shallow and surrounded by barrier reef from the eastward and beach from the west side.

The field observation showed that the beach is sandy and wide, followed by a shallow wide intertidal zone (average 350m in width), then the barrier reef was situated parallel to the shoreline, with an average width of 400m.

2. Abu Ramad site

Abu Ramad is a village from the Halaib Triangle, lies at 125 km south of Shalatein city between latitude 22°24′12.74″ - 22°24′05.43″N and longitude 36°25′16.85″-36°25′16.52″E**.** Its beach is famous with the black sand, especially the downstream of Crav valley. The beach face is sandy, wide (~7m), with a gentle slope and its upper crest delineates the high water level that took place during high tide time. The second prominent zone consists of the rocky narrow intertidal zone with an average width of 50m. This zone is covered by a thin layer of fine sediments and it is characterized by a relatively flat surface. Occasionally, the intertidal zone is exposed during low tide and submerged during high tide up to 0.3m. The considerable narrowness of the tidal flat zone could be attributed to the prolonged accumulation of runoff sediments supplied to the sea from Wadi Crav during the flood periods. The third offshore zone is the back reef area, which varies in depth between 2 and 20m. It is inhabited by some coral patches, and few sea grass spots (Fig. 2F).

Field work

Sediment samples have been collected from Sharm El Madfa and Abu Ramad sites. Surface sediment samples were collected by hand and a grab sampler following the methods of the US Environmental Protection Agency (EPA/CE-81-1 Protocol) for the sample preparation and handling. Three different environmental features; beach, intertidal zone and offshore zone until 20 m water depth represent this location.

Physical and chemical parameters of seawater such as Dissolved Oxygen, Temperature, Total Dissolved Solids, Ion Hydrogen and Salinity were measured in situ using Hanna Instrument (Hi 9828) during the field works. Global Position System GPS (Magellan 1000) recorded the geographic positions. All the submarine photographs were taken with a Sea life Marine Camera.

Laboratory methods

In the laboratory, sediment samples were dried in temperature room for one week. Samples then were homogenized in order to normalize for variations in grain size distribution. The dried sediment samples were packed in clean plastic containers and stored in a dry place until various types of analysis.

1. Determination of moisture content (MC %)

Moisture content is the ratio of the weight of water to the weight of sediment in a given volume of sediment, expressed as a percentage. Moister content is useful when contaminant concentration is to be reported on a dry weight basis, even if determined in wet samples. Moister content was determined according to Loring and Rantala [25]. For water content determination, a known weight of each sample was placed in pre-cleaned and weighed porcelain crucibles. Porcelain crucibles were then placed in an oven previously heated to 85^{o}C and samples were left for 24 hours. Porcelain crucibles were then removed from the oven and placed in a desiccator until reaching room temperature. Finally, Porcelain crucibles were weighed and these steps are repeated until constant weight is reached. The percentage (percentage) of water content was calculated from the following equation: MC% = (WB –WA)/ WB X 100.

Where, MC% = percent of water content, WB= weight of the sample before drying and WA = weight of the sample after drying.

2. Determination of grain size analysis

Grain size determination was made on the dried samples by the usual sieving method according to Folk [26]. About 50 g split of each of the quartered sample was placed into the topmost sieve and the entire column was shaken on a mechanical shaker for about 15 min. The sieve meshes give the class intervals 2000, 1000, 500, 250, 125, and 63 μm.

3. Determination of organic matter content (OM %)

Loss on Ignition (LOI) analysis is used to determine the organic matter content (OM %) of samples. A known weight of each sample was placed in pre-cleaned and weighed porcelain crucibles. Porcelain crucibles were then placed in an oven previously heated to 375^{o}C and samples were left for 16 hours overnight [27-29]. Porcelain crucibles were then removed from the oven and placed in a desiccator until reaching room temperature. Finally, porcelain crucibles were weighed. The percentage (%) of organic matter content was calculated as the difference between the initial and final sample weights divided by the initial sample weight times 100%. All weights had been corrected for moisture content prior to organic matter content calculation.

4. Determination of major and trace elements

A total of 22 ground bulk sediments representing all the samples collected from the two sites in this study were subjected to inductively coupled plasma emission spectrometer (ICP-ES) technique. About 100 g of each sediment were ground to a fine powder and homogenized well, using a cleaned agate mortar and pestle. Chemical analysis was done at Bureau Veritas Minerals (BVM) Laboratories, Canada under the analysis code AQ300 using ICP-ES 34 elements package. The precision of the analyses, based on replicate analysis of digestion solutions, was typically better than ±2 %. Analyses of standard materials indicate that the results are generally accurate to within ± 4-10 %.

5. Environmental assessment

The assessment of heavy metal contamination in sediments is an essential tool to evaluate the risk of an aquatic environment. To identify the pollution and contamination level in the studied coastal sediments, both single and integrated pollution indices were calculated and used to detect the degree of contamination and the sources of metals (Table 1). The single pollution indices include the enrichment factor (EF), geo-accumulation index (Igeo), contamination factor (CF) and anthropogenic fraction (AF).

The integrated pollution indices were represented by contamination degree (Cd), the pollution load index (PLI) and Improved Nemerow Index (I_N). Moreover, statistical (correlation) analyses were performed.

6. Microscopic and X-Ray diffraction (XRD) investigations

For mineralogical investigation, the residual components of the beach sediments at both sites beach were sorted under a binocular microscope at Assiut University, using 40× magnification. The relative percentages of various components of the residues, including carbonate grains (microfossils and/or calcite), detrital grains (rock fragments, heavy minerals, and quartz), ferruginous grains and phosphatic components, were examined and calculated with respect to their volume percent.

A total of 8 samples of ground bulk sediments representing the various sediments in this study were selected for XRD investigation at the Faculty of Science, Assiut University. One sample (AR3 is enriched in heavy minerals) was leached by dilute HCl to dissolve the carbonates and concentrate the heavy minerals fraction.

Results and discussion

1. Sediments characterization

The Sharm El Madfa sediments are sandy in size (Table 2) and are mainly composed of about 30% to 50% of calcareous microfossils including foraminifera, mollusks and some of other shells. Fragmented calcite and/or calcite grains are almost present in these sediments. These grains may represent 40 to70% (by volume percent) of the sediments (Fig. 3A). Quartz grains vary between 5 and 10%. Heavy minerals in most samples of Sharm El Madfa sediments are present in minor percentages (0.1 to 2%) and they consist mainly of ilmenite and magnetite. Minor constituents (0.1 %) of phosphatic components were found in some samples and represented by black crusts and yellow to yellowish brown grains of glassy appearance including fish teeth and fish spines. Fine-to medium- grains of Mn-oxides crusts are also recorded in some samples.

Table 1 Pollution indicators used in the present study and their classifications.

Pollution indicators	Procedures of calculation and classifications
Enrichment factors (EF)	The enrichment factors (EF) were calculated using the formula given by Tribovillard et al. [30]: $EF = (M/Al)_{sample}/(M/Al)_{average\ shale}$ where $(M/Al)_{sample}$ and $(M/Al)_{average\ shale}$ refer, respectively, to the ration of the concentration of the target metal M and Al in the sediment samples and the average shale. The average shale values obtained from Li and Schoonmaker [31]. Birch [32] determined seven classes of EF in sediments: EF < 1 no enrichment; EF < 3 minor enrichment; EF=3–5 moderate enrichment; EF=5–10 moderately severe enrichment; EF=10–25 severe enrichment; EF=25–50 very severe enrichment; EF > 50 extremely severe enrichment
Geo-accumulation Index (I_{geo})	$I_{geo}=Log_2 (C_n/(1.5\times Bn))$ Where C_n is the measured concentration of metal (n) in the sediments, Bn is the geochemical background concentration of the metal (n) in shale, and 1.5 is introduced to minimize the effects of possible variations in the background values. Müller [33] determined seven classes of Igeo in sediments: Igeo < 0 unpolluted; 0 < Igeo < 1 unpolluted to moderately polluted; 1 < Igeo < 2 moderately polluted; 2 < Igeo < 3 moderately to strongly polluted; 3 < Igeo strongly polluted; 4 < Igeo < 5 strongly to very strongly polluted; Igeo > 5 Very strongly polluted Conditions
Contamination Factor (Cf)	$Cf = C_o/C_b$ Where C_o is the sediment metal content in the sample and C_b is the normal background value of the metal. Håkanson [34] classified Cf into four groups: Cf < 1 low contamination factor; 1 ≤ Cf < 3 Moderate contamination factor; 3 ≤ Cf < 6 Considerable contamination factor; Cf ≥ 6 very high contamination factor
Contamination degree (Cd)	$Cd = \sum_{i=1}^{N} Cf$ Where, N is the number of elements analyzed and Cf is the contamination factor calculated. Håkanson [34] classified Cd into four groups: Cd < 8 Low contamination degree; 8 ≤ Cd < 16 Moderate contamination degree; 16 ≤ Cd < 32 Considerable contamination degree; Cd ≥ 32 Very high contamination degree
Pollution Load Index (PLI)	$PLI = (C_{F1}*C_{F2}* C_{F3}*\ldots\ldots C_{F N})^{1/N}$ Where N is the number of metals studied and C_F is the contamination factor calculated. Tomlinson et al. [35] classified the PLI into four groups: PLI < 1 Unpolluted soil; 1 ≤ PLI < 2 Moderated polluted soil; 2 < PLI < 10 Strongly polluted soil; PLI > 10 Extremely polluted soil
Improved Nemerow index (I_N)	$I_N =\sqrt{((I^2_{geomax} + I^2_{geoave}) / 2)}$ I_N is the comprehensive contamination index of a sample; I_{geomax} is the maximum I_{geo} value of such sample and I_{geoave} is the arithmetic mean value of I_{geo} where I_N was calculated for every sampling site using the modified formula given by Guan et al. [36]. Guan et al. [36] classified the I_N into the same seven classes of Igeo with different ranges. $0 > I_N \leq 0.5$ Uncontaminated (Class 0); $0.5 < I_N \leq 1$ Uncontaminated moderately contaminated (Class 1); $1< I_N \leq 2$ moderately contaminated (Class 2); $2 < I_N \leq 3$ moderately–heavily contaminated (Class 3); $3 < I_N \leq 4$ heavily contaminated (Class 4); $4 < I_N \leq 5$ heavily to extremely contaminated (Class 5); $I_N > 5$ Extremely contaminated (Class 6)

The beach sediments at the Abu Ramad site are sandy in size (Table 2) and are chiefly composed of calcareous and quartz grains, k-feldspar, and heavy minerals but with different contents. The sediments of the southern part of the site display calcareous grains (calcite and micro-fossils) of 80% and low content of quartz (5%). In contrast, the sediments of the northern part are more enriched in quartz (70-90%) with lower content in calcareous grains (5-30%). The calcareous grains occur mainly as fragmented calcite and/or micro-fossils and corals. The k-feldspar grains vary between 1 and 5% and are almost correlated with the content of quartz. The heavy minerals display concentrations vary between 3 and 30% with the highest concentrations at samples AR3 and AR1 (Fig. 3B). These grains are represented by ilmenite, magnetite, amphiboles, rutile and zircon in decreasing order (Fig. 3C & D). Few of well rounded reworked phosphatic grains (0.1%) were recorded.

The quartz grains are rounded to well rounded, milky in color and up to 250 μm in size (Fig. 3E). The magnetic grains fraction (magnetite) are very fine to fine grains with grain size varies between 100 to 200 μm (Fig. 3C). Almost of the grains are sub-rounded but some of the finer grains (100 μm) still display idiomorphic habit with octahedral crystals. The ilmenite grains are larger in size than magnetite with grain size varies between 150-350 μm. The grains are sub-rounded to elongated in shape and in some cases display some crystal edges (Fig. 3D). The K-feldspars are represented by rounded to sub-rounded grains of pale pink to pink color and grain size varies between 200 -250 μm but some grains may reach up to 1 mm in size (Fig. 3F). The amphibole grains are pale green in color, rounded to sub-rounded and up to 200 μm in size (Fig. 3D). These detrital grains indicate input of terrigenous fluxes derived from different geographic wadis.

Table 2 Results of grain size analysis and surface water parameters of Sharm El Madfa (Sh) and Abu Ramad (AR) sediments.

	Particle-size (%)							Composition	Surface water parameters			
	> 2mm	> 1mm	> 0.5mm	> 0.25mm	> 0.125mm	> 0.0625mm	Pan		pH	Salinity ‰	DO mg/L	TDS g/L
Sh1	2.56	5.32	7.08	13.16	10.45	45.27	16.17	gravely silty sand	8.13	37.17	14.8	36.40
Sh2	3.18	7.04	14.38	9.06	15.90	42.12	8.33	gravely silty sand	8.07	37.44	15.2	36.73
Sh3	1.64	5.26	4.88	14.04	18.02	47.32	8.86	gravely silty sand	7.96	36.64	12.2	36.22
Sh4	6.05	9.94	14.86	16.72	9.86	32.41	10.15	gravely silty sand	8.04	37.23	12.4	36.53
Sh5	4.61	6.00	7.61	11.52	15.52	49.73	5.02	silty gravely sand	8.04	37.54	14.7	36.86
Sh6	5.20	9.16	12.55	15.19	9.26	44.88	3.76	silty gravely sand	8.01	37.48	14.2	36.79
Sh7	3.24	6.11	11.84	15.71	16.23	42.97	3.90	gravely silty sand	8.01	37	15.6	36.34
Sh8	5.75	14.24	18.44	19.57	10.96	25.46	5.58	gravely silty sand	8	36.27	15.5	58.92
Sh9	0.00	11.08	11.43	13.95	7.89	40.32	15.33	silty sand	8	37.3	14.1	36.6
Sh10	1.98	3.18	16.68	14.36	14.81	42.66	6.34	gravely silty sand	7.99	37.18	12.5	36.47
Sh11	0.00	3.00	10.95	19.78	16.20	30.87	19.20	silty sand	8.06	37.4	14.9	36.73
Sh12	0.00	1.94	11.67	13.48	21.19	50.25	1.48	silty sand	8.08	37.45	15.4	36.73
Sh13	0.00	2.73	18.98	21.84	28.01	24.23	4.21	silty sand	8.13	37.51	14.6	36.79
Sh14	0.00	14.00	26.81	14.63	15.67	21.12	7.76	silty sand	8.09	37.27	16.2	36.6
Sh15	0.00	5.55	27.62	21.73	17.89	21.74	5.47	silty sand	8.12	37.27	12.9	36.53
Sh16	0.00	0.45	10.34	9.63	6.39	38.33	34.86	silty sand	8.08	37.35	14.2	36.6
AR1	0	0.41	0.87	38.67	23.36	34.86	1.84	silty sand	8.18	37.02	12.6	36.34
AR2	0	4.24	14.88	24.57	34.48	18.41	3.42	silty sand	8.07	35.92	14.8	35.23
AR3	0	2.08	2.58	8.07	40.10	44.04	3.14	silty sand	8.3	37.48	9.16	36.73
AR4	2.13	14.60	24.34	32.38	18.26	6.03	2.27	gravely silty sand	8.23	37.11	9.14	36.47
AR5	6.82	14.41	21.08	25.03	24.60	6.10	1.96	silty gravely sand	8.37	36.78	7.12	36.21
AR6	10.18	15.63	22.21	29.32	16.41	6.24	0	gravely sand	8.38	36.88	10.5	36.22

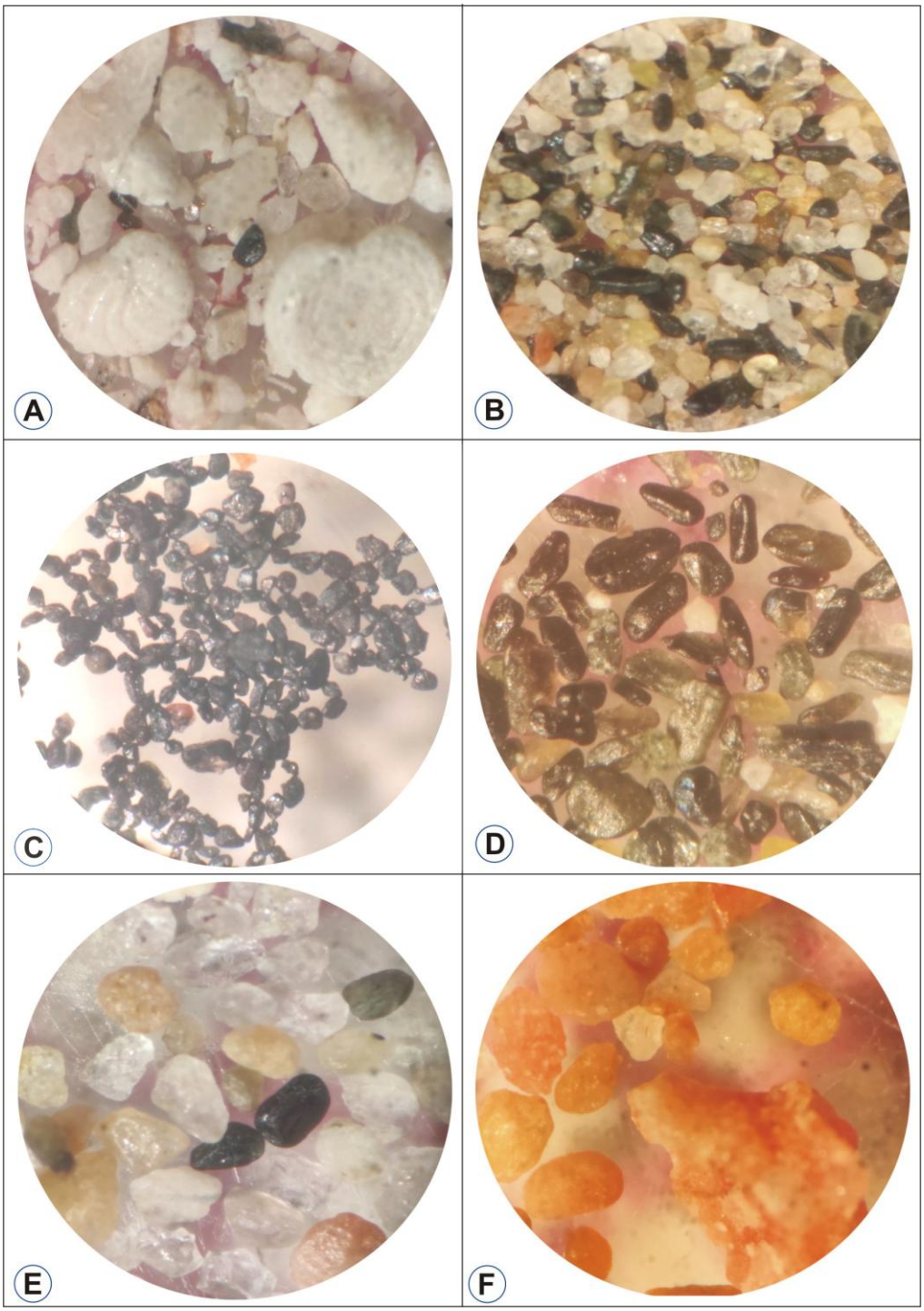

Figure 3. Photomicrographs showing the main composition of the coastal sediments at the two sites, (A) Fragmented calcite and micro-fossils represent the main compositions of the sediments at the two sites, (B) An HCl- leached sediment (sample AR3) displays the main components of black sand at the Abu Ramad site that is composed of sub rounded magnetite grains (C). elongated black grains of ilmenite and light green amphibole (D), milky grains of quartz (E) and pink grains of K-feldspars (F). Field of view is 2.5 mm across in all photos.

2. Physical and chemical parameters of seawater

The seawater at the studied two sites is highly oxygenated due to the saturation and relatively uniform dissolved oxygen (DO) contents, which range from 9.12 to 16.2 mg/L (Table 2). Sharm El Madfa site displays more enriched and almost saturation of DO values which vary between 12.2 and 16.2 mg/L. These minimum and maximum values occur at the southern part of the site (stations Sh19 and Sh18 respectively). At Abu Ramad site, the DO contents show lower values fluctuating between a minimum value of 9.12 mg/L at station AR5 and a maximum value of 14.8 mg/L at station AR2 with almost values between 9 and 10 mg/L. These lower values of DO at Abu Ramd site are attributed to the presence of a mangrove swamp at this site (Fig. 2A & B). The total dissolved salts (TDS) show an identical distribution ranging from 36.22 to 36.8. g/L at Sharm El Madfa samples but one sample (Sh8) exhibits 58.9 g/L (Table 2). Comparable TDS values range between 35.23 and 36.72 g/L are recorded at Abu Ramad Site. The TDS global average is 34.5 g/L [37]. The two sites show additional homogenous pH (8-8.38) and salinity (36- 37.54 ‰) contents.

3. Organic matter content (OM %)

The organic matter contents may show similar values at both Sharm El Madfa and Abu Ramad sites where they exhibit values vary from 0.5 to 4.8% (Table 3). At Sharm El Madfa site, the higher values of OM (2.5- 4%) are relatively associated with the more depth (1.5-3m) samples. They show only a moderate correlation with V and Cr (r=0.6 and 0.5 respectively). At Abu Ramad site, OM content shows values fluctuate between a minimum value of 1% at stations AR1 and AR3 and a maximum value of 4.8% at station AR2 with similar values of 2.5% at the remainder stations (Table 3).

4. Variation of major and trace elements

The results of the ICP-ES elemental analyses of 22 bulk sediments representing all the samples collected from the two sites are given in Table 3. The content of **calcium** in Sharm El Madfa sediments displays irregular distribution along the different samples. It varies from 15 to 33.5%. It shows higher values (28-33.5%) in the southern part (samples; Sh11-Sh16, Fig. 1 and Table 3). It shows a moderate correlation with B (r=0.5) and a good correlation with Sr (r=0.89). They exhibit negative correlations with Ti, Si, k, P, Mn, Zn and La (r= -0.59: -0.97). The Calcium content in Abu Ramad samples displays less concentration than those of Sharm El Madfa. The concentrations vary between 4.23 to 31.6% with the highest values (29-

31.6 %) in the southern part. At this site, Calcium correlates well with Na, S, B and Sr. It is negatively correlated with the remainder of the analyzed elements.

The **silicon** content shows variable values at both sites. It varies between 3.3 and 25.3% in Sharm El Madfa sediments and between 5 and 40% in Abu Ramad samples. It exhibits positive correlations with Ti, P, Mn, Zn and La at Sharm El Madfa site and with Al, Ti, Mn, Cu, Zn and Ni at Abu Ramad site. It shows strong negative correlations with Ca and Mg at both sites.

The **magnesium** content varies between 0.93 and 1.6 % in Sharm El Madfa sediments and between 0.5 to 1.2% in Abu Ramad sediments. It correlates well with Ca, S and Sr. The **sodium** content displays values between 0.5 and 0.66 % in Sharm El Madfa sediments and between 0.32 to 0.56% in Abu Ramad sediments. It correlates well with Mg, Ca and Sr. **Aluminum** varies between 0.12 and 0.33 % in Sharm El Madfa sediments and between 0.1 and 0.57 % in Abu Ramad sediments. It correlates well with Fe, K, Mn, Cu, Ni, V and Cr at Sharm El Madfa site, and with Si, Fe, K, Mn, Cu, Zn, Ni, V, Cr, As, and La at Abu Ramad site. **Iron** varies between 0. 2 and 0.5% in Sharm El Madfa sediments and between 0.1 and 1 % in Abu Ramad sediments. **Sulfur** varies between 0. 2 and 0.34 % in Sharm El Madfa sediments and between 0.06 and 0.16 % in Abu Ramad sediments. The distributions of **Ti, K** and **P** show very low ranges vary between 0.01-0.1% for Ti, 0.03 -0.09% for K and 0.02 - 0.04% for P.

The trace elements analyzed include Mo, Cu, Pb, Zn, Ag, Ni, Co, Mn, As, U, Th, Sr, Cd, Sb, Bi, V, La, Cr, Ba, B, W, Hg, Tl, Ga, and Sc. The results of the trace elements analysis of the studied sites are presented in Table 3. Trace elements such as Mo, Pb, Ag, Co, U, Th, Cd, Sb, Bi, W, Hg, Tl, Ga, and Sc are below the detection limit for all the samples. The detection limits of these elements are 8 ppm (U), 5 ppm (Ga, Sc and Tl), 3 ppm (Pb, Sb and Bi), 2 ppm (Th and W), 1 ppm (Mo, Co, Hg), 0.5 ppm (Cd) and 0.3 ppm (Ag). In contrast, Sr shows values above the upper detection limit (2000 ppm) in more than 50 % of the studied sediments. The relative abundances of the significant trace elements in the studied sediments are as follows: Sr > Mn > B > V > Cr > Ba > Zn > Ni > As > La > Cu (Table 3).

Strontium is the most abundant trace element in the studied Sharm El Madfa and Abu Ramad sediments. It ranges between 482 and > 2000 ppm. It shows a significant correlation with Ca (r= 0.819 and 0.913 at Sharm El Madfa and Abu Ramad

sediments respectively). The lowest values (482 and 863 ppm) were recorded at Abu Ramad site associated with sediments enriched in detrital fraction (feldspars, pyroxenes, amphiboles, magnetite, ilmenite and zircon, Fig. 3). Manganese is the second most abundant trace element detected in the studied sediments. It shows variable content within the sediments of the two sites where it ranges between 31 and 100 ppm at Sharm El Madfa site and 20-196 ppm at Abu Ramad site. Boron displays relatively homogenous values vary between 20 and 35 ppm at the sediments of the two sites. Vanadium varies between 5-10 ppm in Sharm El Madfa sediments and between 6-33 ppm in Abu Ramad sediments. The highest concentration (33 ppm) of V in Abu Ramd is associated with sediments that are enriched in detrital fraction. Chromium content ranges from 4-10 ppm in Sharm El Madfa sediments and from 5-21 ppm in Abu Ramd sediments. Like V, the highest content (21 ppm) of Cr in Abu Ramd is associated with sediments that are enriched in detrital fraction (sample AR3, Table 3). Barium exhibits values between 7 and 16 ppm in the sediments of the two sites. The sediments of the southern part of Sharm El Madfa site display more homogenous values of Ba that vary between 8 and 9 ppm. The zinc content ranges between 2 and 13 ppm in the sediments of the two sites. Nickel, lanthanum and copper show concentration values within the sediments of the two sites range between 2-8, 1-6 and 1- 4 ppm respectively. Arsenic content varies between 2-5 ppm in Sharm El Madfa sediments and between 2-3 ppm in Abu Ramad sediments.

5. Environmental assessment

Enrichment Factors (EF)

The enrichment factor values less than 1.5 indicate that the metal is impoverished relative to the background and is entirely from crustal materials or natural processes. Whereas EF values greater than 1.5 indicate that, the metal is enriched relative to the background and suggest that the sources are more likely to be anthropogenic [38-42].

The calculated EF values for Fe, Mn, Cu, Zn, Ni, As, V and Cr in the Sharm El Madfa and Abu Ramad sediments are presented in Table 4 and their profiles are illustrated in Figure 4.

Table 3 Results of inductively coupled plasma emission spectrometer (ICP-ES) analyses of major and trace elements, and organic matter (OM %) of Sharm El Madfa (Sh) and Abu Ramad (AR) sediments.

	Major elements (%)											Trace elements (ppm)										
	Al	**Ti**	***Si**	**Fe**	**Mg**	**Ca**	**Na**	**K**	**P**	**S**	**OM**	**Cu**	**Zn**	**Ni**	**Mn**	**V**	**As**	**Cr**	**La**	**Ba**	**B**	**Sr**
Sh1	0.14	0.01	19.15	0.19	1.09	18.09	0.56	0.06	0.026	0.19	3	2	13	2	71	5	2	6	3	10	20	1810
Sh2	0.24	0.017	22.20	0.33	1.22	15.73	0.57	0.09	0.037	0.22	4	2	8	3	92	9	3	8	5	12	29	1411
Sh3	0.26	0.02	19.20	0.35	1.15	14.98	0.58	0.09	0.037	0.22	2.5	3	9	4	100	9	2	8	5	15	31	1540
Sh4	0.16	0.013	18.86	0.2	0.93	22.5	0.62	0.06	0.027	0.22	1.5	1	4	2	60	5	2	5	3	14	30	>2000
Sh5	0.2	0.015	21.40	0.25	1.2	17.17	0.56	0.07	0.032	0.21	1.5	1	5	2	83	7	2	7	4	10	21	1508
Sh6	0.14	0.019	9.40	0.2	1.04	32.03	0.55	0.05	0.038	0.15	4	1	2	3	31	10	2	8	1	9	35	2000
Sh7	0.18	0.012	16.26	0.23	1.25	22.52	0.56	0.07	0.032	0.21	0.5	1	4	2	65	6	2	7	3	10	20	1946
Sh8	0.12	0.007	14.97	0.18	1.01	22.42	0.54	0.05	0.027	0.23	1	1	2	1	42	5	4	4	2	10	20	>2000
Sh9	0.22	0.014	21.13	0.33	1.09	18.39	0.5	0.07	0.036	0.2	1	2	8	3	95	7	2	8	5	12	20	1504
Sh10	0.22	0.014	25.25	0.31	0.99	15.14	0.49	0.07	0.034	0.18	4	2	12	3	98	7	2	8	5	12	20	1177
Sh11	0.33	0.012	6.06	0.48	1.56	30.17	0.66	0.09	0.028	0.34	3	3	6	8	72	9	5	10	2	9	28	>2000
Sh12	0.17	0.006	6.19	0.19	1.54	31.56	0.58	0.05	0.021	0.22	1.5	1	2	4	31	5	2	7	1	8	29	>2000
Sh13	0.17	0.006	9.91	0.24	0.94	28.1	0.53	0.05	0.023	0.17	2.5	1	2	4	44	7	3	6	1	8	24	>2000
Sh14	0.16	0.006	3.28	0.18	1.36	33.47	0.51	0.05	0.02	0.21	2	1	4	4	31	5	2	6	1	9	24	>2000
Sh15	0.16	0.006	3.85	0.29	1.07	33.15	0.56	0.05	0.018	0.21	2	1	4	4	37	5	2	6	1	8	30	>2000
Sh16	0.2	0.008	3.96	0.27	1.42	31.26	0.66	0.06	0.023	0.26	2.5	2	6	5	40	6	2	7	1	16	32	>2000
AR1	0.24	0.018	39.79	0.33	0.49	4.23	0.32	0.05	0.018	0.06	1	2	7	3	196	10	3	7	3	16	20	482
AR2	0.19	0.015	21.00	0.2	1.04	18.04	0.39	0.04	0.031	0.12	4.8	2	10	4	32	7	2	7	2	7	20	>2000
AR3	0.57	0.096	37.23	0.99	0.81	5.81	0.32	0.06	0.035	0.06	1	4	13	8	125	33	3	21	6	13	20	863
AR4	0.07	0.007	5.08	0.1	1.2	31.61	0.48	0.03	0.03	0.15	2.5	1	1	2	20	6	2	5	1	7	27	>2000
AR5	0.12	0.016	6.62	0.21	1.17	30.79	0.56	0.04	0.024	0.16	2.5	1	2	3	33	9	2	7	2	8	35	>2000
AR6	0.12	0.018	8.30	0.2	1.04	29.11	0.54	0.05	0.038	0.15	2.5	1	3	3	32	9	2	7	2	8	35	>2000

Enrichment factors show higher values for all metals (EF > 1.5). However, only some samples display low enrichment (EF < 1.5) for Cu and very few samples for Zn in the two sites. The average values of the calculated EF for trace elements in the Sharm El Madfa sediments are as follows: As (9) > Cr (3.6) > Mn (3.34) > Ni (3.1) > Zn (2.76) > Fe (2.56) > V(2.43) > Cu (1.57). The sediments of Abu Ramada site display average values of EF as follows: As (10.18) > Cr (4.74) > V (4.2) > Ni (3.7) > Mn (3.51) > Fe (2.8) > Zn (2.48) > Cu (1.8). These values of EF indicate that these metals are slightly to moderately severe enriched relative to the background and suggest that at least some fractions of the sources of these metals are more likely to be anthropogenic. However, some samples in the two sites display no enrichment (EF < 1.5) for, Zn, and Cu indicating lithogenic origin.

The Sharm El Madfa sediments show enrichment factor for As varies from 5.21 to 22.57 with almost values lie between 6 and 10. Only one sample shows EF of 22.57. The As EF values at Abu Ramad site vary between 3.6 and 19.2 with almost values range between 7-11. The highest EF is recorded in sample AR4. Cr is moderately enriched in Sharm El Madfa sediments with EF values vary between 3 and 4.2. It shows severe enrichment in Abu Ramad sediments with EF values between 3 and 7. The EF values of V and Mn lie between 1.9 and 5 in Sharm El Madfa sediments. The values range between 2.5-5.8 and 1.7-8.5 for V and Mn in Abu Ramad sediments respectively. Ni is slightly to moderately enriched at the two sites with EF values range between 1.5- 4.4 and 2.2-5 at Sharm El Madfa and Abu Ramad sediments respectively. Zn and Cu vary significantly in their enrichment in the two sites. They vary from no enrichment (EF < 1.5), slightly enrichment (EF= 1.5- 3) and severe enrichment (EF= 5-8.6 for Zn). Fe shows slightly to moderately enrichment in the two sites with EF values ranging between 2 and 3.4.

Table 4 Enrichment factor (EF), geo-accumulation index (Igeo), contamination factor (CF), anthropogenic fraction (AF %), contamination degree (Cd), pollution load index (PLI) and improved nemerow index (I_N) of heavy metals in the sediments of the studied sites.

	Fe	Mn	Cu	Zn	Ni	As	V	Cr	
EF of Sharm El Madfa site									
Min.	2.09	1.89	0.98	1.09	1.47	5.21	1.85	2.96	
Max.	3.38	5.25	2.80	8.60	4.40	22.57	4.84	5.59	
Aver.	2.56	3.34	1.57	2.76	3.07	9.03	2.43	3.62	
EF of Abu- Ramad site									
Min.	1.96	1.74	1.37	1.32	2.20	3.56	2.49	2.85	
Max.	3.27	8.46	2.80	4.88	5.03	19.34	5.80	6.98	
Aver.	2.80	3.51	1.85	2.48	3.70	10.18	4.20	4.74	
I_{geo} and I_N of Sharm El Madfa site									***I_N***
Min.	-5.30	-6.78	-6.08	-6.15	-6.23	-3.29	-5.29	-5.08	3.1
Max.	-3.88	-5.32	-4.49	-3.45	-3.23	-1.96	-4.29	-3.75	4.3
Aver.	-4.80	-6.15	-5.57	-4.90	-4.63	-3.07	-4.91	-4.31	4
I_{geo} and I_N of Abu- Ramad site									***I_N***
Min.	-5.30	-6.37	-6.08	-6.15	-4.23	-3.29	-5.29	-4.49	3.12
Max.	-3.88	-5.32	-4.49	-4.57	-3.23	-1.96	-4.44	-3.75	4.29
Aver.	-4.77	-6.11	-5.65	-5.29	-4.01	-2.97	-5.02	-4.29	3.97
CF and Cd of Sharm El Madfa site									***Cd***
Min.	0.04	0.04	0.02	0.02	0.02	0.15	0.01	0.04	0.44
Max.	0.10	0.12	0.07	0.14	0.16	0.39	0.04	0.11	1.01
Aver.	0.06	0.07	0.03	0.06	0.07	0.19	0.02	0.08	0.58
CF and Cd of Abu- Ramad site									***Cd***
Min.	0.02	0.02	0.02	0.01	0.04	0.15	0.01	0.06	0.34
Max.	0.21	0.23	0.09	0.14	0.16	0.23	0.07	0.23	1.27
Aver.	0.07	0.09	0.04	0.06	0.08	0.18	0.03	0.10	0.64
AF% and PLI of Sharm El Madfa site site									***PLI***
Min.	52.01	45.16	-2	8.2	31.6	80.5	45.73	66.34	0.04
Max.	70.41	80.28	64.3	88.37	77.2	95.5	79.28	82.15	0.10
Aver.	60.43	65.39	30.94	52.15	62.79	87.46	56.78	71.81	0.06
AF% and PLI of Abu- Ramad site									***PLI***
Min.	49.05	40.63	27.33	24.40	54.40	71.50	59.83	65.03	0.027
Max.	69.35	87.76	64.30	79.48	80.05	94.75	82.73	85.72	0.146
Aver.	63.13	62.32	43.26	51.92	70.20	87.00	73.67	76.73	0.066

Geo-accumulation index (Igeo)

The results of Igeo values for all elements in the studied two sites exhibit very low values (< 0) indicating unpolluted sediments (Table 4)**.**

Contamination factor (Cf) and contamination degree (Cd)

The assessment of sediment contamination was also carried out using the contamination factor (Cf) and the degree of contaminations (Cd) of Håkanson [34]. The data of these two indices are tabulated in Table 4. According to Håkanson [34] (Table 1), the overall samples of sediments at the two sites, based on the Cf and Cd values show low contamination factors for both Cf and Cd.

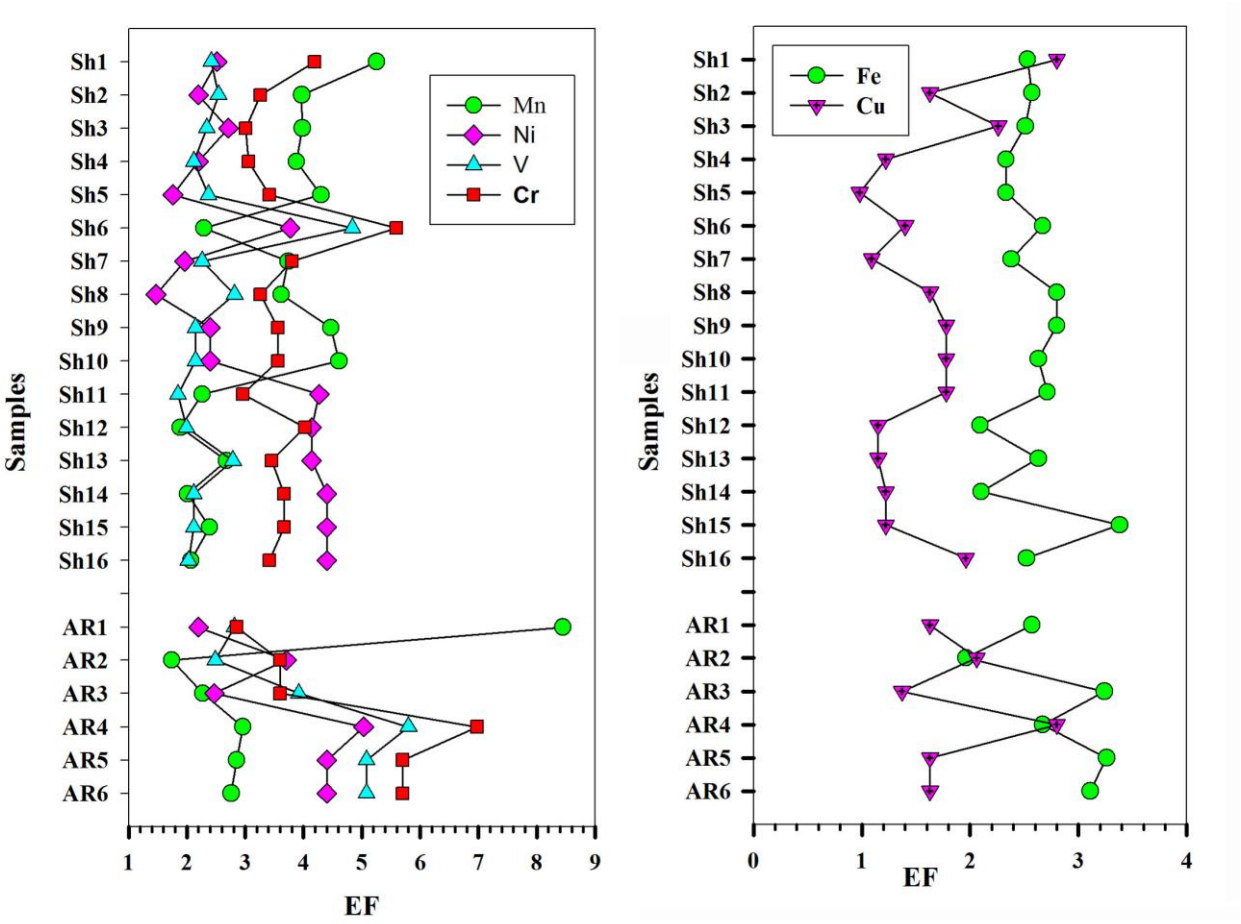

Figure 4. Heavy element enrichement factors (EF) in Sharm El Madfa (Sh) and Abu Ramad (AR) coastline sediment samples.

The pollution load index (PLI)

The pollution load index (PLI) was used to recognize multi-metal contamination. In this study, PLI is calculated for eight heavy metals in each sample in the two sites using the equation adopted by Tomlinson et al. [35] (Table 1). The PLI values range from 0.03 to 0.15 (Table 4) confirming that the sediments at the studied two sites are in unpolluted condition.

Improved Nemerow Index (I_N)

The evaluation of the single pollution indices are only for a single heavy metal contaminant, thus these indices cannot provide a comprehensive description of the contamination status of an area [36]. Therefore, an evaluation based on the comprehensive index method is necessary. Improved Nemerow Index (I_N, Guan et al. [36] was developed by replacing the single factor index with Igeo (Table 1).

The improved Nemerow index (I_N) is calculated as the sum of eight heavy metals (Table 4). The I_N results of all sampling points in the two sites indicate the following. (1) In general, the I_N values at the two sites range between 3 and 5 (classes 3-5), with the minimum and maximum values between 2.93 and 4.62. These values indicate that the overall level of heavy metal contamination in the studied two sites is between heavily and extremely contaminated, which indicates serious heavy metal contamination. (2) Only one sample at Abu Ramad site displays I_N value less than 3 (2.93, class 3) indicating moderately to heavily contamination. (3) The I_N values of 10 samples from 16 samples at Sharm El Madfa site and 4 samples from 6 samples at Abu Ramad site exceed 4, which indicate that the contamination level is extremely contaminated. (4) These high levels of contamination are not concentrated in any specific area but show uneven distribution at the two sites.

The anthropogenic fraction (AF)

The enrichment factor index (EF) is a convenient measurement to predict the source of heavy metals (lithogenic or anthropogenic). Therefore, the total levels of heavy metals in all studied sediments (EF > 1.5, Table 4 and Fig. 4) are generally high and come from lithogenic and anthropogenic sources.

Anthropogenic pollution is the introduction by humans into the environment of polluting elements that alter their quality causing a negative effect. The resources of anthropogenic pollution are varied, the major ones being the ones related to industrial and urban activities. Anthropogenic pollution can be physical, chemical and biological, with serious consequences for natural ecosystems and for the human being himself. It produces a large extinction of biodiversity and the deterioration of ecosystems essential to human survival.

According to Uwah et al. (2013), the *Lithogenic* fraction of element X in a sample can be estimated as; *Lithogenic* $X = (X/Al)_{average\ shale} \times Al_{sample}$. The anthropogenic fraction (AF) of a heavy metal can be estimated by the formula: Total X – *Lithogenic* X. However, this definition is the same of Tribovillard et al. [30] for the determination of authigenic fraction where: detrital $X= (X/Al)_{average\ shale} \times Al_{sample}$. The authigenic fraction of element X is calculated as total X −detrital X. Therefore, this definition of the anthropogenic/authigenic fraction comprises all biogenic, anthropogenic and early diagenetic processes that take place at very shallow depth (few centimeters) under the water/sediments interface.

The anthropogenic component of the total concentration of an element (C_{AC}) was estimated by Vale et al. [43] using the following expression:

$CAC= [(C_{ele} / C_{Al}) – (C_{PI} / C_{Al\text{-}pI})] / (C_{ele}/C_{Al}) \times C_{ele}$

Where C_{ele} is the present-time concentration of the element normalized to the aluminum content (C_{Al}) and C_{PI} is the pre-industrial level found in deep layers of sediment cores in the Tagus Estuary [44] divided by the corresponding Al content $C_{Al\text{-}pI}$). In this study, all sediments are surface sediments, therefore we used the values of the elements and the corresponding Al content in average shale instead of ($C_{PI} / C_{Al\text{-}pI}$) of Vale et al. [43]. The estimation of anthropogenic fraction (AF) by using both of the equations of Vale et al., [43] and Uwah et al. [45] gives identical values.

The calculated AF percentages for Fe, Mn, Cu, Zn, Ni, As,V and Cr in the Sharm El Madfa and Abu Ramad sediments are displayed in Table 4. The anthropogenic fraction show various percentages among all metals at the sediments of both sites. The average values of the calculated AF for trace elements in the Sharm El Madfa sediments are as follows: As (87.46%) > Cr (71.81%) > Mn (65.39) > Ni (62.79%) > Fe (60.43%) > V(56.78%) > Zn (52.15%) > Cu (30.94%). The sediments of Abu Ramada site exhibit average values of AF as follows: As (87%) > Cr (76.73%) > V(73.67%) > Ni (70.19%) > Fe (63.13%) > Mn (62.32) > Zn (51.92%) > Cu (43.26%).

The anthropogenic fraction of As at Sharm El Madfa sediments varies from 83 to 96% with the almost values lying between 85 and 88%. Only one sample shows AF of 95.5%. The AF values of As at Abu Ramad site vary between 72 and 95%. The highest values of AF (91-95%) are recorded at the southern part of the site. The AF of Cr shows similar percentages in the sediments of the two sites with values range between 67-82% and 85-86% at Sharm El Madfa and Abu Ramad sediments respectively. The southern parts of the two sites display relatively the highest concentrations of AF. Similar values of AF of Mn are recorded in the sediments of the two sites with concentrations range from 45-80% at Sharm El Madfa site and 41-86% at Abu Ramad site. The highest values of AF of Mn are recorded at the northern and southern parts of Sharm El Madfa and Abu Ramad sediments respectively. The AF of V shows lower values at the Sharm El Madfa sediments with concentrations ranging between 46 and 79% and relatively higher values at Abu Ramad sediments range

between 64-83%. The southern part of Abu Ramad sediments displays the highest content of AF for V with a relatively similar content of 80-83%. The content of AF of Ni is similar to that of V where the Sharm El Madfa sediments display the lower concentration (32-77%) and Abu Ramad sediments display the higher values (54-80%). The southern parts of the two sites display the highest concentrations of AF of Ni (Table 4). The anthropogenic fraction of Fe shows variable content within the sediments of the two sites where it ranges between 52 and 70 % at Sharm El Madfa site with most values range between 60 and 64% and only one sample displays 70%. At Abu Ramad site, the anthropogenic fraction of Fe shows values between 49 and 69 %. However, most of the iron in these sediments may show a significant association with the detrital fraction of heavy minerals such as magnetite, Ti-carrier phases and ± chromite (Fig. 3). Zn and Cu are vary significantly in their concentrations in AF in the sediments of the two sites. The Sharm El Madfa sediments display AF contents of Zn and Cu vary between 8-88% and 8-64% respectively. However, Abu Ramad sediments show values of AF for Zn and Cu range between 24-79% and 27-64% respectively. The distributions of AF of the two elements within the sediments are not concentrated in any specific area but show uneven distribution at the two sites.

Correlation analysis

In order to estimate the interrelationship between elements in Sharm El Madfa and Abu Ramad sediments, Pearson correlation coefficients are calculated (Tables 5 and 6). As shown in Tables 5 and 6, most of the analyzed metals are correlated positively with each other.

At Sharm El Madfa site, significantly positive correlations were observed between Al and each of Fe, K, Cr, Cu, Ni, S, Mn, V, and As (r= 0.942, 0.872, 0.831, 0.815, 0.692, 0.641, 0.619, 0.604 and 0.417, respectively, Table 5). Also, significantly positive correlations between Fe and each of K, Cr, Cu, Ni, S, Mn, V, and As (r = 0.797, 0.784, 0.801, 0.688, 0.6 03, 0.581,0.598 and 0.478, respectively). Mn is also correlated well with both of Zn (r = 0.745) and Cu (r= 0.643). S shows a positive correlation with each of the heavy metals Cu, Ni and As (r= 0.513, 0.654, and 0.650 respectively).

At Abu Ramad Site, the elements Al, Si, Fe, Ti and K show a significant positive correlation among each other's with correlation coefficients (r) vary between 0.593 and 0.99. These elements (Al, Si, Fe, Ti and K) show strong positive correlations with the heavy metals Mn, Cu, Zn, Ni, V, Cr and As (r vary between 0.793-0.983, 0.592-

0.931, 0.761-0.992, 0.665-0.998 and 0.673-0.783 respectively, Table 6). Manganese exhibits significant correlations with each of Cu (r= 0.569), Zn (r = 0.505) and As (0.947).

These positive correlations among a group of elements referring to be that all of these elements are well associated with each other and were originated from the same source. The correlation between the heavy metals Cr, Cu, Ni, V, and As with both of Al and Fe (± Si and Ti) indicates that these metals are associated with the detrital charier phases produced by natural weathering processes and/or absorbed by iron oxides. This relation is well evident at the Abu Ramad Site where the sediments are enriched in detrital phases such as quartz, magnetite, ilmenite, rutile, amphiboles, K-feldspar and zircon (Fig. 3). The correlation of some elements such as S with Cu, Ni, and As, and Mn with Cu and Zn suggests that these elements are partly occur as fine sulfides and partly scavenging by Mn-oxides and or hydroxides.

However, the improved nemerow index (IN) results of all sampling points in the two sites indicate that the overall level of heavy metal contamination in the studied two sites is between heavily and extremely contaminated**.** The enrichment factors of the heavy metals (Fe, Mn, Cu, Zn, Ni, As, V and Cr,) in all studied sediments (EF > 1.5) are generally high and come from lithogenic and anthropogenic sources. Consequently, the calculated anthropogenic fraction (AF) for Fe, Mn, Cu, Zn, Ni, As,V and Cr in the Sharm El Madfa and Abu Ramad sediments show various percentages among all metals at the sediments of both sites.

The possible anthropogenic sources of these metals are paints used to protect coastal structures and ships against fouling and corrosive, shipment operations and shipyards. Other sources include dredging and land filling in wadi entrances, pipes, and other industrial sources. As well as, the studied sites receive variable amounts of municipal wastewater from tourist centers and from fishermen and cargo boats. Pouring sewage and wastewater directly on the beach (Fig. 2).

Table 5 Correlation matrix among analyzed metals of Sharm El Madfa sediments.

	Al	Ti	Si	Fe	Mg	Ca	Na	K	P	S	Mn	Cu	Zn	Ni	V	Cr	As	La	B	Ba	Sr	OM
Al	1.000																					
Ti	0.421	1.000																				
Si	0.131	0.616	1.000																			
Fe	0.942	0.369	0.091	1.000																		
Mg	0.456	-0.198	-0.507	0.297	1.000																	
Ca	-0.238	-0.588	-0.965	-0.189	0.397	1.000																
Na	0.372	0.009	-0.355	0.318	0.509	0.275	1.000															
K	0.872	0.660	0.480	0.797	0.245	-0.589	0.287	1.000														
P	0.362	0.929	0.713	0.327	-0.254	-0.671	-0.185	0.618	1.000													
S	0.641	-0.135	-0.308	0.603	0.678	0.180	0.735	0.470	-0.203	1.000												
Mn	0.619	0.666	0.830	0.581	-0.164	-0.887	-0.134	0.826	0.699	0.070	1.000											
Cu	0.815	0.440	0.216	0.801	0.284	-0.371	0.335	0.796	0.386	0.513	0.643	1.000										
Zn	0.375	0.373	0.584	0.372	-0.096	-0.665	-0.116	0.538	0.361	-0.002	0.745	0.680	1.000									
Ni	0.692	-0.115	-0.583	0.688	0.640	0.489	0.509	0.310	-0.236	0.654	-0.082	0.542	-0.013	1.000								
V	0.604	0.777	0.199	0.598	0.039	-0.203	0.102	0.616	0.744	0.050	0.417	0.517	0.137	0.350	1.000							
Cr	0.831	0.550	0.063	0.784	0.462	-0.093	0.201	0.692	0.510	0.326	0.475	0.674	0.343	0.638	0.765	1.000						
As	0.417	-0.124	-0.163	0.478	0.227	0.106	0.317	0.295	-0.032	0.650	0.006	0.315	-0.168	0.430	0.266	0.179	1.000					
La	0.444	0.687	0.909	0.396	-0.263	-0.937	-0.258	0.725	0.743	-0.081	0.961	0.486	0.685	-0.299	0.333	0.326	-0.126	1.000				
B	0.136	0.219	-0.472	0.142	0.215	0.469	0.572	0.020	-0.029	0.154	-0.338	0.117	-0.297	0.440	0.382	0.239	-0.053	-0.353	1.00			
Ba	0.283	0.434	0.377	0.208	-0.081	-0.451	0.337	0.436	0.364	0.164	0.458	0.483	0.432	-0.057	0.133	0.088	-0.245	0.490	0.21	1.00		
Sr	-0.407	-0.588	-0.800	-0.371	0.228	0.819	0.417	-0.582	-0.653	0.220	-0.863	-0.419	-0.702	0.212	-0.363	-0.396	0.207	-0.894	0.33	-0.36	1.00	
OM	0.278	0.390	0.076	0.306	-0.063	-0.066	0.031	0.261	0.304	-0.118	0.177	0.410	0.421	0.307	0.601	0.472	0.103	0.105	0.38	0.07	-0.33	1.00

Table 6 Correlation matrix among analyzed metals of Abu Ramad sediments.

	Al	Ti	Si	Fe	Mg	Ca	Na	K	P	S	Mn	Cu	Zn	Ni	V	Cr	As	La	B	Ba	Sr	OM
Al	1																					
Ti	0.964	1.000																				
Si	0.780	0.593	1.000																			
Fe	0.986	0.990	0.694	1.000																		
Mg	-0.530	-0.333	-0.913	-0.457	1.000																	
Ca	-0.782	-0.594	-0.999	-0.693	0.903	1.000																
Na	-0.728	-0.537	-0.940	-0.623	0.791	0.948	1.000															
K	0.810	0.777	0.711	0.812	-0.659	-0.705	-0.508	1.000														
P	0.191	0.361	-0.288	0.241	0.444	0.271	0.217	0.209	1.000													
S	-0.806	-0.637	-0.991	-0.732	0.899	0.989	0.950	-0.706	0.242	1.000												
Mn	0.581	0.405	0.909	0.529	-0.975	-0.894	-0.783	0.637	-0.514	-0.909	1.000											
Cu	0.983	0.919	0.809	0.945	-0.532	-0.817	-0.808	0.734	0.172	-0.832	0.569	1.000										
Zn	0.865	0.742	0.815	0.776	-0.540	-0.832	-0.831	0.673	0.153	-0.796	0.505	0.923	1.000									
Ni	0.964	0.971	0.619	0.960	-0.315	-0.628	-0.582	0.758	0.375	-0.639	0.356	0.947	0.855	1.000								
V	0.961	0.998	0.602	0.992	-0.359	-0.601	-0.534	0.783	0.319	-0.649	0.440	0.909	0.714	0.954	1.000							
Cr	0.965	0.999	0.592	0.988	-0.323	-0.594	-0.536	0.771	0.360	-0.632	0.393	0.923	0.756	0.978	0.995	1.000						
As	0.793	0.665	0.931	0.761	-0.893	-0.920	-0.833	0.739	-0.300	-0.956	0.947	0.773	0.643	0.604	0.694	0.653	1.000					
La	0.987	0.963	0.765	0.989	-0.556	-0.763	-0.662	0.871	0.167	-0.788	0.613	0.944	0.806	0.944	0.967	0.962	0.811	1.000				
B	-0.594	-0.398	-0.812	-0.470	0.619	0.828	0.957	-0.272	0.203	0.819	-0.602	-0.717	-0.790	-0.481	-0.383	-0.403	-0.649	-0.491	1.000			
Ba	0.614	0.462	0.889	0.579	-0.956	-0.872	-0.743	0.684	-0.470	-0.895	0.994	0.583	0.485	0.394	0.500	0.448	0.960	0.657	-0.540	1.00		
Sr	-0.682	-0.527	-0.926	-0.639	0.945	0.913	0.821	-0.675	0.423	0.942	-0.987	-0.668	-0.565	-0.467	-0.560	-0.514	-0.985	-0.705	0.639	-0.99	1.00	
OM	-0.145	-0.249	-0.043	-0.268	0.225	0.011	-0.125	-0.292	0.135	0.120	-0.357	-0.002	0.336	-0.017	-0.309	-0.218	-0.396	-0.253	-0.339	-0.44	0.39	1.00

Conclusions

The present study focused on the assessment of the contamination levels of selected heavy metals of the Sharm El Madfa and Abu Ramad coastal sediments, Red Sea, Egypt.

Assessment of heavy metals pollution in sediments was evaluated using enrichment factor (EF), geo-accumulation index (Igeo), contamination factor (CF), anthropogenic fraction (AF), contamination degree (Cd), the pollution load index (PLI) and Improved Nemerow Index (I_N).

The coastal sediments collected from the two sites have shown average metal levels in the following order: Ca > Si > Mg > Na > Fe > S > Al > K > Ti > P> Sr > Mn > B > V > Cr > Ba > Zn > Ni > As > La > Cu.

The geo-accumulation index, contamination factor, contamination degree and pollution load index showed that the sediments at both sites were unpolluted.

The calculated EF values for the heavy metals Fe, Mn, Cu, Zn, Ni, As,V and Cr in the Sharm El Madfa and Abu Ramad sediments show higher values for all metals (EF > 1.5). The average values of the calculated EF for trace elements in the Sharm El Madfa sediments are as follows: As (9) > Cr (3.6) > Mn (3.34) > Ni (3.1) > Zn (2.76) > Fe (2.56) > V(2.43) > Cu (1.57). The sediments of Abu Ramada site display average values of EF as follows: As (10.18) > Cr (4.74) > V (4.2) > Ni (3.7) > Mn (3.51) > Fe (2.8) > Zn (2.48) > Cu (1.8). These values of EF indicate that these metals are slightly to moderately enriched relative to the background and suggest that at least some fractions of the sources of these metals are more likely to be anthropogenic.

The improved Nemerow index (I_N) data of all sampling points in the two sites indicate the following. (1) In general, the I_N values at the two sites range between 3 and 5 (classes 3-5), with the minimum and maximum values between 2.93 and 4.62. These values indicate that the overall level of heavy metal contamination in the studied two sites is between heavily and extremely contaminated, which indicates serious heavy metal contamination. (2) The I_N values of 10 samples from 16 samples at Sharm El Madfa site and 4 samples from 6 samples at Abu Ramad site exceed 4, which indicate that the

contamination level is extremely contaminated. (4) These high levels of contamination are not concentrated in any specific area but show uneven distribution at the two sites.

The calculated anthropogenic fraction percentages for Fe, Mn, Cu, Zn, Ni, As,V and Cr in Sharm El Madfa and Abu Ramad sediments show variable percentages among all metals at the sediments of both sites. The correlation between the heavy metals with both of Al and Fe (± Si and Ti) indicates that these metals are associated with the detrital charier phases and/or absorbed by iron and Mn-oxides and or hydroxides. The possible anthropogenic sources of these metals are shipment operations and anticorrosive and antifouling paints, dredging and land filling in wadi entrances, pipes, municipal wastewater from tourist centers and fishermen cargo boats.

References

[1] F. Fu and Q. Wang, Removal of heavy metal ions from wastewaters: a review. J Environ Manage, vol. 92, pp. 407–418, 2011

[2] A. S. El-Sorogy, M. Abdel-Wahab, A. Ziko, and W. Shehata, Impact of some trace metals on bryozoan occurrences, Red Sea coast, Egypt. Indian J Geomar Sci. vol. 45, pp. 86–99, 2016

[3] Z. Zhaoyong, Y. Xiaodong, and Y. Shengtian, Heavy metal pollution assessment,source identification, and health risk evaluation in Aibi Lake of northwest China. Environ Monit Assess, vol. 190, 69, 2018

[4] M. Martinez-Colon, P. Hallock, and C. Green-Ruiz, Strategies for using shallow-water benthic foraminifers as bioindicators of potentially toxic elements: a Review. J. Foram Res. Vol. 39, pp. 278–299, 2009, doi:10.2113/gsjfr.39.4.278

[5] M. Youssef, Heavy metals contamination and distribution of benthic foraminifera from the Red Sea coastal are, Jeddah, Saudi Arabia. Oceanologia, vol. 57, pp. 236-250**,** 2015

[6] A. M. El-Sabbagh, M. I. Ibrahim, A. R. Mostafa, N. O. Al-Habshi, and M. R. Abdel Kireem, Benthic foraminiferal proxies for pollution monitoring in Al-mukalla coastal area, Hadramout Governate, Republic of Yemen. J, Foram Res. vol. 46, pp. 369–392, 2016

[7] D. O'Rourke and S. Connolly, Just oil? the distribution of environment and social impacts of oil production and consumption. Annu Rev Environ Resour, vol. 28, pp. 587-617, 2003

[8] H. W. Nuremberg, The voltammetric approach in trace metal chemistry of natural waters and atmospheric precipitation. Anal Chim Acta, vol. 164, pp. 1–21, 1984

[9] U. Forstner, Contaminated sediments. Lecture notes in earth science, 21st edn. Springer-Verlag, Berlin 157 pp, 1990

[10] J. Harte, C. Holdren, R. Schneider, and C. Shirley, Toxics A to Z, a guide to everyday pollution hazards. University of California Press, Oxford, 478 pp. 1991

[11] G. Schuurmann and B. Market, Ecotoxicology, ecological fundamentals, chemical exposure, and biological effects. John Wiley & Sons Inc, and Spektrum Akademischer Verlag, 936 pp. 1997

[12] F. Ahmadipour, N. Bahramifar, and S.M. Ghasempouri, Fractionation and mobility of cadmium and lead in soils of Amol area in Iran, using the modified BCR sequential extraction method. Chem Speciat Bioavailab, vol. 26, pp. 31–36, 2014

[13] M. Abd El-Wahab and A. S. El-Sorogy, Scleractinian corals as pollution indicators, Red Sea coast, Egypt. N Jb Geol Paläont Mh, vol. 11, pp. 641–655, 2003

[14] A. S. El-Sorogy, M. Abdelwahab, and H. Nour, Heavy metals contamination of the quaternary coral reefs, Red Sea coast, Egypt. Environ Earth Sci, vol 67, pp. 777–785, 2012

[15] A. S. El-Sorogy, A. El Kammar, A. Ziko, M. Aly, and H. Nour, Gastropod shells as pollution indicators, Red Sea coast, Egypt. J Afr Earth Sci, vol. 87, pp. 93–99, 2013

[16] O. E. Attia and H. Ghrefat, Assessing heavy metal pollution in the recent bottom sediments of Mabahiss Bay, North Hurghada, Red Sea, Egypt. Environ Monit Assess, vol. 185(12), pp. 9925–9934, 2013

[17] A. R. A. Usman, R. S. Alkredaa, and M. I. Al-Wabel, Heavy metal contamination in sediments and mangroves from the coast of Red Sea: Avicennia marina as potential metal bioaccumulator. Ecotoxicol Environ Saf, vol. 97, pp. 263–270, 2013

[18] D. M. Salem, A. Khaled, A. El Nemr, and A. El-Sikaily, Comprehensive risk assessment of heavy metals in surface sediments along the Egyptian Red Sea coast. Egypt J Aqua Res, vol. 40, pp. 349–362, 2014

[19] M. Youssef and A. S. El-Sorogy, Environmental assessment of heavy metal contamination in bottom sediments of Al-Kharrar lagoon, Rabigh, Red Sea, Saudi Arabia Arab J Geosci, vol. 9, 474, 2016

[20] H. Nour, A. S. El-Sorogy, M. Abdel-Wahab, S. Almadani, H. Alfaifi, and M. Youssef, Assessment of sediment quality using different pollution indicators and statistical analyses, Hurghada area, Red Sea coast, Egypt. Mar Pollut Bull, vol. 133, pp. 808–813, 2018

[21] H. Nour, A. S. El-Sorogy, M. Abd El-Wahab, and M. M. Nouh El Said Al-Kahtany, Contamination and ecological risk assessment of heavy metals pollutionfrom the Shalateen coastal sediments, Red Sea, Egypt. Marine Pollution Bulletin, vol. 144(2019), pp, 167 172, 2019

[22] A. Kahal, A. S. El-Sorogy, H. Alfaifi, S. Almadani, and H. A. Ghrefat, Spatial distribution and ecological risk assessment of the coastal surface sediments from the Red Sea, northwest Saudi Arabia. Mar Pollut Bull, vol. 137, pp. 198–208, 2018

[23] Y. Kim, B. K. Kim, and K. Kim, Distribution and speciation of heavy metals and their sources in Kumho River sediment, Korea. Environ.Earth Sci, vol. 60(5), pp. 943-952, 2009

[24] M. Nowrouzi and A. Pourkhabbaz, Application of geoaccumulation index and enrichment factor for assessing metal contamination in the sediments of Hara Biosphere Reserve, Iran. Chemical Speciation and Bioavailability, vol. 26(2), pp. 99-105, 2014

[25] D. H. Loring and R. T. T. Rantala, Manual for the geochemical analyses of marine sediments and suspended particulate matter. Earth Science Reviews, vol. 32, pp. 235-283, 1992

[26] R. L. Folk, Petrology of Sedimentary Rocks. Hemphill, Austin, pp 184, 1980

[27] L. J. Blume, P. W. Schumacher, K. A. Shaffer, K. A. Cappo, and M. L. Papp, Handbook of methods for acid-deposition studies. Laboratory analyses for soil chemistry. pp348. EPA/600/4-90/023. U.S. Environmental Protection Agency, Las Vegas, 1990

[28] D. W. Nelson and L. E. Sommers, Total carbon, organic carbon, and organic matter. In: Methods of Soil Analysis, Part 2, 2nd ed, AL Page et al. Ed. Agronomy, vol. 9, pp. 961-1010. Am. Soc. of Agron, Inc. Madison WI., 1996

[29] ASTM, Standard test methods for moisture, ash, and organic matter of peat and other organic soils. Method D 2974-00. American Society for Testing and Materials. West Conshohocken, US, 2000

[30] N. Tribovillard, T. J. Algeo, T. Lyons, and A. Riboulleau, Trace metals as paleoredox and paleoproductivity proxies: An update. Chem Geol, vol. 232, pp. 12-32, 2006

[31] Y. H. Li and J. E. Schoonmaker, Chemical composition and mineralogy of marine sediments. In: Holland HD, K. K.Turekian (Eds), Treatise on Geochemistry. Elsevier Ltd pp. 3469–3503, 2003

[32] G. Birch, A scheme for assessing human impacts on coastal aquatic environments using sediments. In: Woodcoffe, CD, Furness, RA. (Eds), Coastal GIS Wollongong University Papers in Center for Maritime Policy 14 Australia, 2003

[33] G. Müller, Die schwermetallbelastung der sediment des Neckars und Seiner Nebenflusse: eine Bestandsaufnahme. Chemical Zeitung, vol. 105, pp. 157–164, 1981

[34] L. Håkanson, An ecological risk index for aquatic pollution control. A sedimentological approach. Water Res, vol. 14, pp. 975–1001, 1980

[35] D. L. Tomlinson, J. G. Wilson, C. R. Hariis, and D. W. Jeffrey, Problems in the assessment of heavy metal levels in estuaries and the formation of a pollution index. Helgoländer Meeresunters, vol. 33, pp. 566-575, 1980

[36] Y. Guan, C. Shao, and M. Ju, Heavy Metal Contamination Assessment and Partition for Industrial and Mining Gathering Areas. International Journal of Environmental Research and Public Health, vol. 11, pp. 7286-7303, 2014, doi:10.3390/ijerph110707286

[37] K. Gaid and Y. Treal, Le dessalement des eaux par osmose inverse: l'expérience de Véolia Water Desalination, vol. 203,, pp. 1–14, 2007, doi.org/10.1016/j.desal.2006.03.523

[38] R. F. Nolting, W. Helder, H. J. W. Baar, and L. J. A. Gerringa, Contrasting behavior of trace metals in the Scheldt estuary in 1978 compared to recent years. Journal of Sea Research, vol. 42, pp. 275–290, 1999

[39] J. Zhang, and C. L. Liu, Riverine composition and estuarine geochemistry of particulate metals in China—weathering features anthropogenic impact and chemical fluxes. Estuarine, Coas and Sh Sci, vol. 54, pp. 1051–1070, 2002

[40] H. Feng, X. Han, W. Zhang, and L. Yu, A Preliminary Study of Heavy Metal Contamination in Yangtze River Intertidal Zone Due to Urbanization. Marine Pollution Bulletin, vol. 49, pp. 910-915, 2004, http://dx.doi.org/10.1016/j.marpolbul.2004.06.014

[41] S. G. Tuncel, S. Tugrul, and T. Topal, A case study on trace metals in surface sediments and dissolved inorganic nutrients in surface water of Oludeniz Lagoon Mediterranean, Turkey. Water Research, vol. 41, pp. 365–372, 2007

[42] C. Nikolaidis, I. Zafiriadis, V. Mathioudakis, and T. Constantinidis, Heavy metal pollution associated with an abandoned lead-zinc mine in the Kirki region, NE Greece. Bulletin of Environmental Contamination and Toxicology, vol. 85(3), pp. 307–312, 2010

[43] C. Vale, J. Canàrio, M. Caetano, J. Lavrado, and P. Brito, Estimation of the anthropogenic fraction of elements in surface sediments of the Tagus Estuary (Portugal). Marine Pollution Bulletin, vol. 56, pp. 1353–1376, 2008

[44] C. Vale, Temporal variations of particulate metals in the Tagus River Estuary. Science of the Total Environment, vol. 97(98), pp. 137–154, 1990

[45] I. E. Uwah, S. F. Dan, R. A. Etiuma, and U. E. Umoh, Evaluation of Status of Heavy Metals Pollution of Sediments in Qua-Iboe River Estuary and Associated Creeks, South-Eastern Nigeria. Environment and Pollution, vol. 2(4), 2013, doi:10.5539/ep.v2n4p110.